Science
AAAS

Unimpeded Permeation of Water Through Helium-Leak–Tight Graphene-Based Membranes

R. R. Nair, *et al.*

Science **335**, 442 (2012);
DOI: 10.1126/science.1211694

Science (print ISSN 0036-8075; online ISSN 1095-9203) is published weekly, except the last week in December, by the American Association for the Advancement of Science, 1200 New York Avenue NW, Washington, DC 20005.

Unimpeded Permeation of Water Through Helium-Leak–Tight Graphene-Based Membranes

R. R. Nair,[1,2] H. A. Wu,[1,3] P. N. Jayaram,[2] I. V. Grigorieva,[1] A. K. Geim[1,2]*

Permeation through nanometer pores is important in the design of materials for filtration and separation techniques and because of unusual fundamental behavior arising at the molecular scale. We found that submicrometer-thick membranes made from graphene oxide can be completely impermeable to liquids, vapors, and gases, including helium, but these membranes allow unimpeded permeation of water (H_2O permeates through the membranes at least 10^{10} times faster than He). We attribute these seemingly incompatible observations to a low-friction flow of a monolayer of water through two-dimensional capillaries formed by closely spaced graphene sheets. Diffusion of other molecules is blocked by reversible narrowing of the capillaries in low humidity and/or by their clogging with water.

Despite being only one atom thick, graphene is believed to be impermeable to all gases and liquids (*1*, *2*), which makes it tempting to exploit this material as a barrier film. Because of the ways graphene can currently be mass produced (*3*), films made from graphene oxide (GO) present a particularly interesting candidate. By using this graphene derivative, it is possible to make laminates, which are a collection of micron-sized GO crystallites forming an interlocked layered structure (*4*–*6*). This structure resembles that of nacre and exhibits great mechanical strength and flexibility, even for films of submicron thickness (*3*–*6*). In this Report, we investigate molecular permeation through such films.

Figure 1A shows an example of the studied GO membranes that were prepared as follows (*7*): We employed Hummer's method to obtain graphite oxide that was dispersed in water by sonication to make a stable suspension of GO crystallites (*4*–*6*). We then used this suspension to produce laminates by spray- or spin-coating (*7*). Scanning electron microscopy and x-ray analysis reveal that such GO films have a pronounced layered structure (Fig. 1B) and consist of crystals with typical sizes L of a few micrometers, which are separated by a typical distance d of ~10 Å (*4*–*6*). For permeation experiments, Cu foils of several centimeters in diameter were uniformly covered with the GO laminates. Then, we chemically etched Cu to produce apertures of diameter $D \approx 1$ cm fully covered by freestanding GO films (fig. S1). Finally, a metal container was sealed by using the Cu disks (fig. S2). We studied membranes with thicknesses h from 0.1 to 10 μm. Even submicrometer-thick membranes were strong enough to withstand a differential pressure ΔP up to 100 mbar.

As an initial test, we filled the containers with various gases under a small overpressure (<100 mbar) and recorded its changes over a period of several days. We observed no noticeable reduction in ΔP for any tested gas including He, H_2, N_2, and Ar. This allowed an estimate for the upper limit on their permeation rates Pr as $\approx 10^{-11}$ g/cm^2·s·bar, which is close to the value reported for micron-sized "balloons" made from continuous graphene monolayers (*1*). In an alternative approach, we used mass spectrometry (fig. S2) and found no detectable permeation of He (Fig. 1D). The accuracy was limited only by digital noise of our He spectrometer and a slightly fluctuating background, which yielded $Pr < 10^{-12}$ g/cm^2·s·bar. Using hydrogen mass spectrometry, no permeation was found either, albeit the accuracy was three orders of magnitude lower than for He, due to a larger background. A 12-μm-thick film of polyethylene terephthalate (PET) was used as a reference barrier and exhibited a He leakage rate 1000 times higher than our detection limit (Fig. 1D) yielding PET's bulk permeability $\prod_{He} = Pr \cdot h \approx 10^{-11}$ mm·g/cm^2·s·bar, in agreement with literature values. The measurements set up an upper limit on $\prod_{He}$ for GO laminates as $\approx 10^{-15}$ mm·g/cm^2·s·bar; that is, our submicrometer-thick films provide a higher He gas barrier than 1-mm-thick glass (*8*).

To evaluate the permeation barrier for liquid substances, we employed weight-loss measurements. Figure 2 shows examples for evaporation rates from a metal container with an aperture covered by a 1-μm-thick GO membrane. No weight loss could be detected with accuracy of <1 mg for ethanol, hexane, acetone, decane, and propanol in the measurements lasting several days (*7*). This sets an upper limit for their $\prod$ as $\approx 10^{-11}$ mm·g/cm^2·s·bar. Unexpectedly, we observed a huge weight loss if the container was filled with water. Moreover, the evaporation rate was practically the same as in the absence of the GO film; that is, for the open aperture (Fig. 2A and fig. S3).

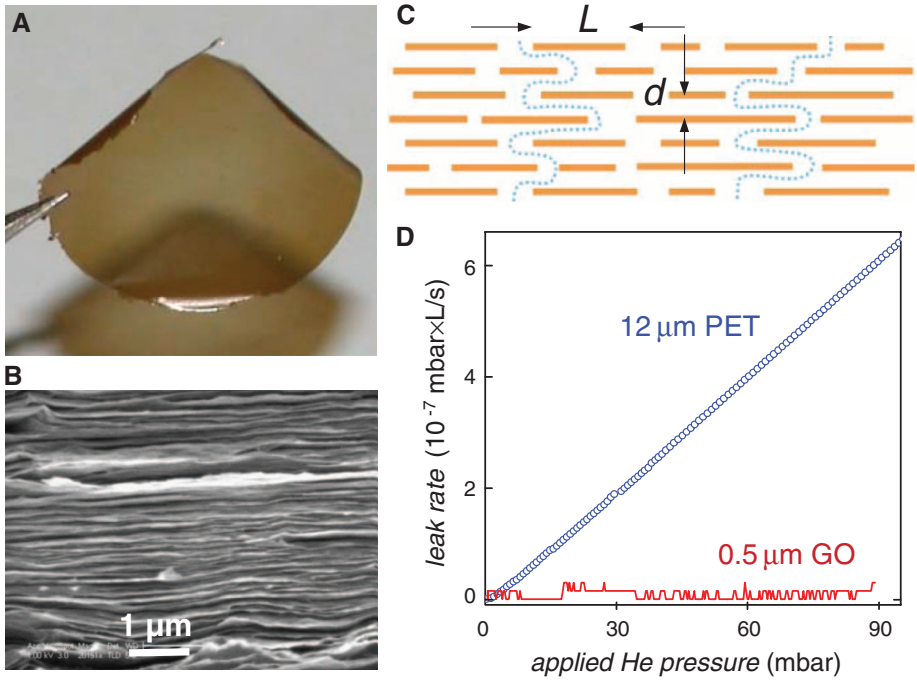

Fig. 1. He-leak–tight GO membranes. (**A**) Photo of a 1-μm-thick GO film peeled off of a Cu foil. (**B**) Electron micrograph of the film's cross section. (**C**) Schematic view for possible permeation through the laminates. Typical L/d is ~1000. (**D**) Examples of He-leak measurements for a freestanding submicrometer-thick GO membrane and a reference PET film (normalized per square centimeter).

[1]School of Physics and Astronomy, University of Manchester, Manchester M13 9PL, UK. [2]Centre for Mesoscience and Nanotechnology, University of Manchester, Manchester M13 9PL, UK. [3]Department of Modern Mechanics, Chinese Academy of Sciences Key Laboratory of Mechanical Behavior and Design of Materials, University of Science and Technology of China, Hefei, Anhui 230027, China.

*To whom correspondence should be addressed. E-mail: geim@manchester.ac.uk

The latter was confirmed directly by using the same aperture with and without a GO cover. Furthermore, the same membrane could be used many times for different liquids, always exhibiting unimpeded and zero evaporation for H_2O and other molecules, respectively. Also, after measurements with water, we checked the membranes for a He leak and found none. Only if we increased h to several micrometers could we observe a partial inhibition of water evaporation from the container (fig. S5), which yielded $\prod_{H2O} \approx 10^{-5}$ mm·g/cm^2·s·bar; that is, water permeates through GO films more than 10 orders of magnitude faster than He (Fig. 2B).

To elucidate the origin of the fast transport of water vapor through otherwise leak-tight GO films, we have carried out a number of additional experiments. First, we reduced GO by annealing it at 250°C in a hydrogen-argon atmosphere (*5*). The membranes became fragile and required extreme care to avoid cracks but nonetheless became 100 times less permeable to water (Fig. 2A). This can be attributed to structural changes such that d decreased from ≈10 to 4 Å, as shown by x-ray analysis and in agreement with earlier reports (*9*, *10*). The importance of the interlayer distance was also witnessed when the partial pressure of water inside the container was reduced (fig. S3). If the pressure dropped below 10 mbar, the permeation stopped (*7*), which again can be explained by changes in d in low humidity. X-ray analysis of GO in various humidity shows that this blockage occurs when d falls below ≈7 Å (*11*, *12*). The process of opening and closing the GO capillaries was found reversible with varying humidity (*7*).

Further insights into the permeation mechanism come from experiments using mixtures of H_2O with other gases and liquids. Mass spectroscopy showed that, in the presence of saturated water vapor, He did permeate through GO membranes (fig. S4). However, its rate was ≈five orders of magnitude slower than that of H_2O, in agreement with the rate calculated for He diffusion through an equivalent column of water (*7*). For other molecules (for example, ethanol and H_2), we were unable to detect their permeation along with H_2O (*7*). This shows that, despite somewhat larger d in high humidity, the intercalating water blocks, or at least impedes, other molecules from moving through GO.

In another series of experiments, we investigated why water permeated through GO film as fast as through an open aperture. To this end, membranes were placed on a support grid that allowed us to apply a water pressure of several bars without damaging them. The large ΔP did not result in any noticeable increase in Pr with respect to water vapor. On the other hand, if we increased humidity outside the container, Pr decreased. Furthermore, if we blew air at the GO membrane, this increased the weight loss rate. Also, Pr increased if the container was heated (we could increase temperature up to 40°C, above which the membranes had a tendency to develop cracks). The same changes in Pr happened when we changed temperature of the membrane only, without heating water inside. In all the cases, Pr changed similarly to the evaporation rate from an open-water surface under similar conditions. This suggests that permeation of water through our membranes was limited by evaporation from the wetted surface of GO.

To explain our findings, we recall that GO laminates consist of crystallites stacked on top of each other (Fig. 1C). The groups (for instance, hydroxyl, epoxy, etc.) attached to graphene sheets are responsible (*9*–*12*) for keeping the relatively large spacing d (fig. S6). Importantly, such groups tend to cluster and leave large, percolating regions of graphene sheets not oxidized (*5*, *7*, *13*, *14*). Therefore, GO laminates are likely to have empty spaces formed between nonoxidized regions of graphene sheets (fig. S6). Because d for reduced GO is ≈4 Å, the empty space's width δ can be estimated as ≈5 Å, which is sufficient to accommodate a monolayer of water (*15*, *16*). We speculate that these empty spaces form a network of pristine-graphene capillaries within GO laminates. By invoking the same water-permeation mechanism as previously used for small-diameter carbon nanotubes and hydrophobic nanopores (*17*–*25*), we suggest that the two-dimensional (2D) graphene nanocapillaries allow low-friction flow of monolayer water. At the same time, the oxidized regions that strongly interact with intercalating water are unlikely (*7*) to contribute to water permeation and, in our model, serve as spacers for the 2D capillary network (fig. S6).

To support our explanation, we used molecular dynamics (MD) simulations (*7*). Because a graphene monolayer is essentially impermeable, molecular transport in GO laminates should involve a permeation path through the network of graphene nanocapillaries as discussed above (Fig. 1C and fig. S6). The bottleneck in this process is the passage between graphene sheets separated by $d << L$ (figs. S6 and S7). For $d \leq 6$ Å (including the van der Waals thickness of graphene), our MD simulations show that water cannot fill the capillaries. On the other hand, for $d \geq 10$ Å, two layers of water start forming between the sheets. For intermediate d, water rushes into the capillaries (*21*, *22*) and forms a highly ordered monolayer shown (Fig. 2B, inset), in agreement with the previous analysis for 2D capillaries (*15*, *16*). Furthermore, the simulations enabled us to estimate the involved capillary pressure as on the order of 1000 bars (*7*), in qualitative agreement with the estimates based on van der Waals interaction between water and graphite (*26*). Such capillary pressures explain why the water permeation in our experiments was insensitive to ΔP of several bars. Similar to the case of nanotubes, our simulated water can move anomalously fast, with velocities reaching meters per second and, thus, sufficient to sustain the observed permeation rates (fig. S8). Finally, we mimicked the oxidized graphene regions by adding arrays of epoxy groups to the simulated capillaries and found the water permeation being strongly impeded for all $d \leq 10$ Å.

The observed unimpeded evaporation of water through He-leak–tight membranes resembles the permeation of protons (atomic hydrogen) through thin films of transition metals, a phenomenon known as superpermeability (*27*). Despite the analogy, our phenomenon is different and explained by a network of graphene nanocapillaries formed within GO laminates, which are filled with monolayer water under ambient conditions. A capillary-like pressure provides a sufficient flow to keep the external GO surface wetted so that the observed permeability is effectively limited by the surface evaporation (*28*). The described GO membranes can be used as barrier films in the design of filtration and separation materials and for selective removal of water (*7*).

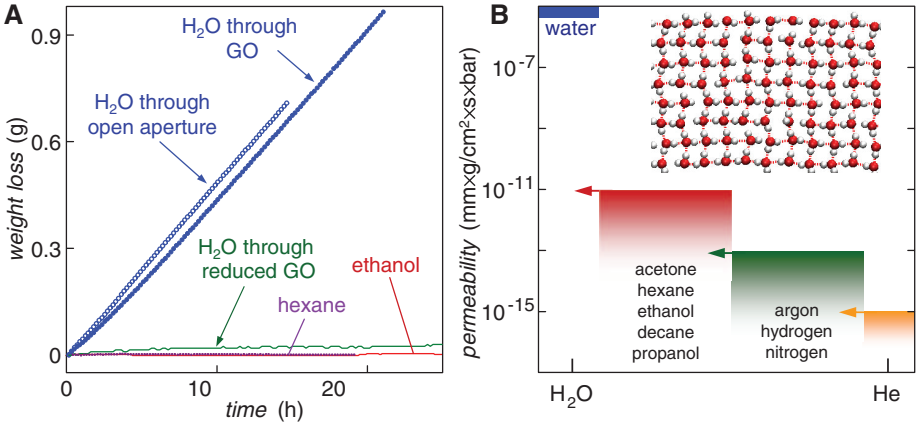

Fig. 2. Permeation through GO. (**A**) Weight loss for a container sealed with a GO film ($h \approx 1$ μm; aperture's area ≈ 1 cm^2). No loss was detected for ethanol, hexane, etc. (*7*), but water evaporated from the container as freely as through an open aperture (blue curves). The measurements were carried out at room temperature in zero humidity. (**B**) Permeability of GO paper with respect to water and various small molecules (arrows indicate the upper limits set by our experiments). (Inset) Schematic representation of the structure of monolayer water inside a graphene capillary with $d = 7$ Å, as found in our MD simulations (*7*).

References and Notes

1. J. S. Bunch *et al.*, *Nano Lett.* **8**, 2458 (2008).
2. O. Leenaerts, B. Partoens, F. M. Peeters, *Appl. Phys. Lett.* **93**, 193107 (2008).
3. A. K. Geim, *Science* **324**, 1530 (2009).
4. D. A. Dikin *et al.*, *Nature* **448**, 457 (2007).
5. G. Eda, M. Chhowalla, *Adv. Mater.* **22**, 2392 (2010).
6. J. T. Robinson *et al.*, *Nano Lett.* **8**, 3441 (2008).
7. See supporting material on *Science* Online.
8. F. J. Norton, *J. Am. Ceram. Soc.* **36**, 90 (1953).
9. M. J. McAllister *et al.*, *Chem. Mater.* **19**, 4396 (2007).
10. H. K. Jeong *et al.*, *Chem. Phys. Lett.* **470**, 255 (2009).
11. A. Lerf *et al.*, *J. Phys. Chem. Solids* **67**, 1106 (2006).
12. S. Cerveny, F. Barros-Bujans, Á. Alegría, J. Colmenero, *J. Phys. Chem. C* **114**, 2604 (2010).
13. N. R. Wilson *et al.*, *ACS Nano* **3**, 2547 (2009).
14. D. Pacilé *et al.*, *Carbon* **49**, 966 (2011).
15. R. Zangi, A. E. Mark, *Phys. Rev. Lett.* **91**, 025502 (2003).
16. N. Giovambattista, P. J. Rossky, P. G. Debenedetti, *Phys. Rev. Lett.* **102**, 050603 (2009).
17. J. K. Holt *et al.*, *Science* **312**, 1034 (2006).
18. M. Majumder, N. Chopra, R. Andrews, B. J. Hinds, *Nature* **438**, 44 (2005).
19. X. Peng, J. Jin, Y. Nakamura, T. Ohno, I. Ichinose, *Nat. Nanotechnol.* **4**, 353 (2009).
20. X. Qin, Q. Yuan, Y. Zhao, S. Xie, Z. Liu, *Nano Lett.* **11**, 2173 (2011).
21. M. Whitby, N. Quirke, *Nat. Nanotechnol.* **2**, 87 (2007).
22. J. C. Rasaiah, S. Garde, G. Hummer, *Annu. Rev. Phys. Chem.* **59**, 713 (2008).
23. J. Köfinger, G. Hummer, C. Dellago, *Proc. Natl. Acad. Sci. U.S.A.* **105**, 13218 (2008).
24. J. A. Thomas, A. J. H. McGaughey, *Phys. Rev. Lett.* **102**, 184502 (2009).
25. Y. Li, J. Xu, D. Li, *Microfluid. Nanofluid.* **9**, 1011 (2010).
26. F. Caupin, M. W. Cole, S. Balibar, J. Treiner, *Europhys. Lett.* **82**, 56004 (2008).
27. A. I. Livshits, M. E. Notkin, V. I. Pistunovich, M. Bacal, A. O. Busnyuk, *J. Nucl. Mater.* **220-222**, 259 (1995).
28. N. Goedecke, J. Eijkel, A. Manz, *Lab Chip* **2**, 219 (2002).

Acknowledgments: This work was supported by the Engineering and Physical Research Council (UK), the U.S. Office of Naval Research, the U.S. Air Force Office of Scientific Research, the Royal Society, and the Körber Foundation. We thank K. S. Novoselov, E. Hill, P. Blake, S. Neubeck, and R. Joshi for their help. H.A.W. is grateful for support from the National Science Foundation of China and Oversea Academic Training Funds–University of Science and Technology of China.

Supporting Online Material

www.sciencemag.org/cgi/content/full/335/6067/442/DC1
Materials and Methods
SOM Text
Figs. S1 to S8
References (*29*–*38*)

25 July 2011; accepted 17 November 2011
10.1126/science.1211694

Ultrafast Viscous Permeation of Organic Solvents Through Diamond-Like Carbon Nanosheets

Santanu Karan,[1] Sadaki Samitsu,[1] Xinsheng Peng,[1]* Keiji Kurashima,[1] Izumi Ichinose[1,2]†

Chemical, petrochemical, energy, and environment-related industries strongly require high-performance nanofiltration membranes applicable to organic solvents. To achieve high solvent permeability, filtration membranes must be as thin as possible, while retaining mechanical strength and solvent resistance. Here, we report on the preparation of ultrathin free-standing amorphous carbon membranes with Young's moduli of 90 to 170 gigapascals. The membranes can separate organic dyes at a rate three orders of magnitude greater than that of commercially available membranes. Permeation experiments revealed that the hard carbon layer has hydrophobic pores of ~1 nanometer, which allow the ultrafast viscous permeation of organic solvents through the membrane.

About 40 years ago, reverse-osmosis membranes applicable to seawater desalination were prepared by plasma polymerization of organic monomers (*1*). Membranes obtained from hydrophilic monomers showed high salt rejection and water permeability (*2*, *3*). The permeation mechanism was discussed in terms of the free-volume theory of polymers (*4*, *5*) or the hydrodynamic flow of water through micropores. However, initial expectations for the use of plasma-polymerized membranes gradually diminished with the improved performance of cross-linked polyimide membranes (*6*). Today, asymmetric polyimide membranes are mass-produced for organic solvent nanofiltration by the phase-inversion method. Meanwhile, thin supported carbon membranes made by various techniques are mainly used for gas separations (*7*, *8*).

Diamond-like carbon (DLC) was also made ~40 years ago by Aisenberg and Chabot (*9*). They prepared thin transparent films very similar to diamond by means of an ion-beam deposition technique. Currently, a widely used technique for DLC deposition is plasma chemical vapor deposition using organic compounds (*10*, *11*). In plasma polymerization of organic compounds, a highly cross-linked network of sp^3 carbons is obtained under certain conditions, which provides the resulting thin carbon films with mechanical stability broadly comparable to diamond. We have become interested in the process by which molecules permeate through such a highly cross-linked molecular network. By improving the permeability, we can thereby obtain extremely hard and thin carbon membranes with great advantages for separation technologies.

We demonstrate the ultrafast permeation of organic solvents through DLC nanosheets, free-standing amorphous carbon membranes with thicknesses ranging from 10 to 40 nm. In addition to their high permeability for various solvents, the membranes have excellent separation performance for organic solutes. Interestingly, the solvent flux was mainly affected by the viscosity of the solvents, not by their molecular size or dipole moment.

We prepared the uniform ultrathin DLC membrane on a sacrificial layer of cadmium hydroxide nanostrands (*12*) by using a parallel-plate plasma-enhanced chemical vapor deposition reactor [radio frequency (RF) power: 5 to 50 W at 13.56 MHz, deposition time: 10 to 370 s, pressure: 1 to 6 Pa] (figs. S1 to S3). To prevent damage of the nanostrands, the substrate temperature was maintained at –20°C. We carefully removed the sacrificial layer by treating it with an ethanolic solution of hydrochloric acid (Fig. 1, C to F). The configuration of the filtration membrane is shown in Fig. 1A. In this case, a 35-nm DLC membrane is formed on a 200-nm-pore alumina support. The membrane has a relatively porous layer of thickness ~10 nm where removal of the nanostrands occurred. However, the overall membrane was completely defect-free, as observed by scanning electron microscopy (SEM), and could be used for high-pressure filtration up to at least 2.0 MPa. Nano-indentation measurements confirmed that the membrane prepared from acetylene diluted in argon gas (RF power: 50 W) has a Young's modulus of 170 GPa and a hardness of 20.1 GPa (Table 1). In this case, the Young's modulus is one-seventh the elastic modulus of diamond (1050 to 1200 GPa) (*13*). Solid-state ^{13}C cross-polarization/magic angle spinning nuclear magnetic resonance (CP/MAS NMR) measurements revealed that the membrane contains 47% sp^3 carbons and 53% sp^2 carbons (fig. S4) (*14*). High-resolution transmission electron microscopy (HRTEM) observations confirmed that the acetylene membrane produced at a low substrate temperature (–20°C) was a typical hydrogenated amorphous carbon (a-C:H soft) (fig. S5) (*15*). Fourier-transform infrared measurements indicated the membrane has a relatively high hydrogen content (fig. S6). Furthermore, we estimated the carbon content to be 95.6 atomic % by x-ray photoelectron spectroscopy (XPS) (fig. S7 and table S1). Deconvolution of the C_{1S} spectra indicated that some of the carbon atoms had been oxidized to form ether (or alcohol), carbonyl, and ester (or carboxyl) groups. Based on these data, the internal chemical structure of the acetylene membrane is presumed to be as shown in Fig. 1B.

DLC membranes made from pyridine and hexamethyldisiloxane (HMDS) gave high elastic moduli of 106 and 91.8 GPa, respectively, and

[1]Polymer Materials Unit, National Institute for Materials Science, 1-1 Namiki, Tsukuba, Ibaraki 305-0044, Japan. [2]Japan Science and Technology Agency (JST), Core Research for Evolutional Science and Technology (CREST), 5 Sanbancho, Chiyoda-ku, Tokyo 102-0075, Japan.

*Present address: Department of Materials Science and Engineering, Zhejiang University, Hangzhou 310027, China.
†To whom correspondence should be addressed. E-mail: ichinose.izumi@nims.go.jp